

Supporting Information

Colloidal Quantum Dot Chains: Self-Assembled Mechanism and Ratiometric

Qin Sun,^{a,b,c} Liang Yang,^{a,b,c} Lei Su,^{a,b,c} Weikang Liu,^a Yifan Wang,^a Shaoming Yu, Changlong Jiang,^{*,a,b,c} and Zhongping Zhang^{a,c,d}

^aCAS Center for Excellence in Nanoscience, Institute of Intelligent Machines, Chinese Academy of Sciences, Hefei, Anhui 230031, China

^bDepartment of Chemistry, University of Science and Technology of China, Hefei, Anhui 230026, China.

^cState Key Laboratory of Transducer Technology, Chinese Academy of Sciences, Hefei, Anhui 230031, China.

^dSchool of Chemistry and Chemical Engineering, Anhui University, Hefei, Anhui 230601, China

*To whom correspondence should be addressed. E-mail: cljiang@iim.ac.cn. Fax: (+86) 551-65591156.

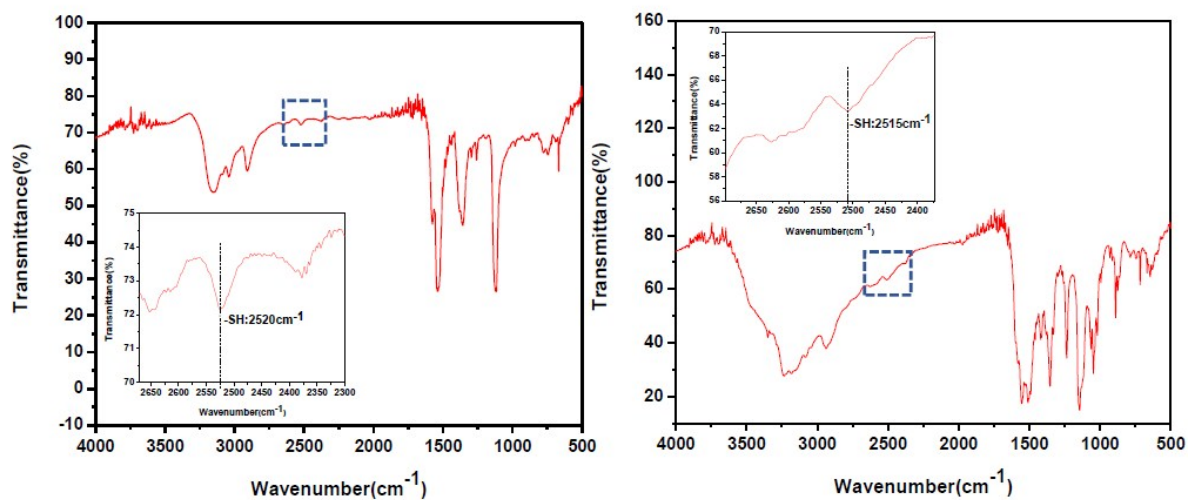


Figure S1. FTIR spectra of TTCA (left) and TTCA-QDs (right)

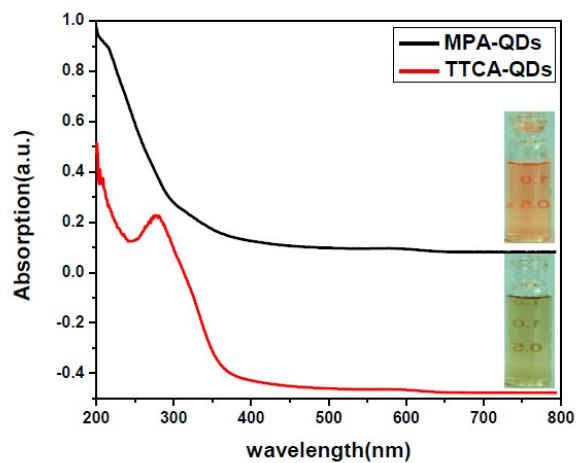


Figure S2. The normalized absorption spectra of MPA-QDs and TTCA-QDs. Inserts are the corresponding digital photos.

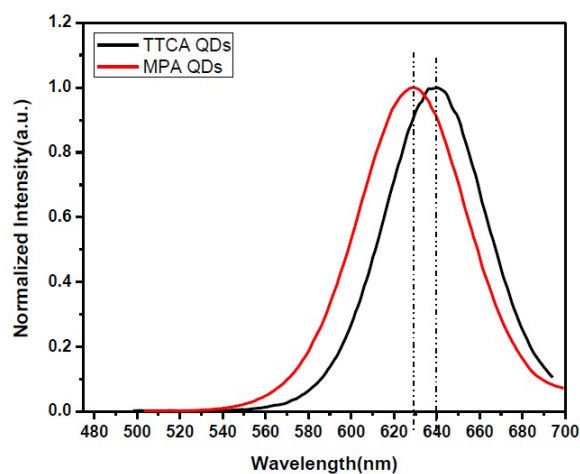


Figure S3. The normalized fluorescent intensity of TTCA-QDs and MPA QDs respectively.

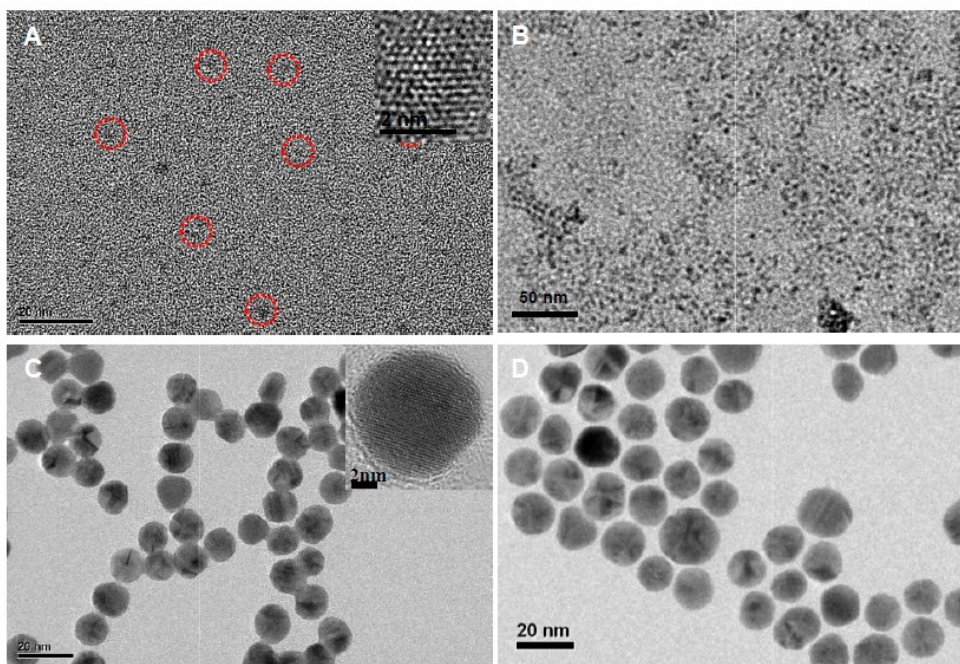


Figure S4. TEM images of the nanocrystals with different sizes. The green-emission QDs with the size of about 2 nm without (A) and with the treatment of TTCA(B), Au nanoparticles with the size of about 12 nm without (C) and with the treatment of TTCA(D). Insert HRTEM images in A and C indicate the nice crystalline essence of the QDs and Au NPs

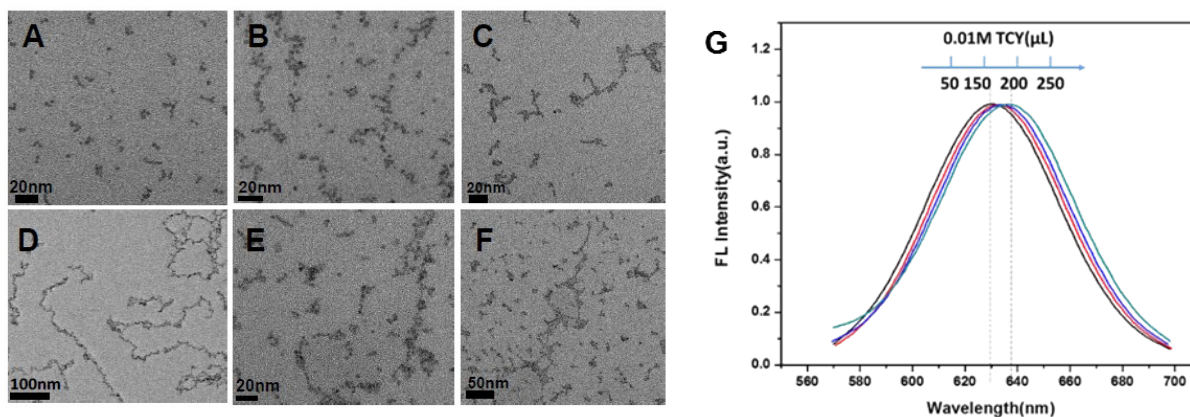


Figure S5. TEM image of TTCA-QDs for different amounts of TTCA used in the experiments. (A) 50 μL 0.01 M; (B) 150 μL 0.01 M; (C) 200 μL 0.01 M; (D) 250 μL 0.01 M; (E) 300 μL 0.01 M; (F) 400 μL 0.01 M. (G) The Fluorescent spectra of different QDs assemblies.

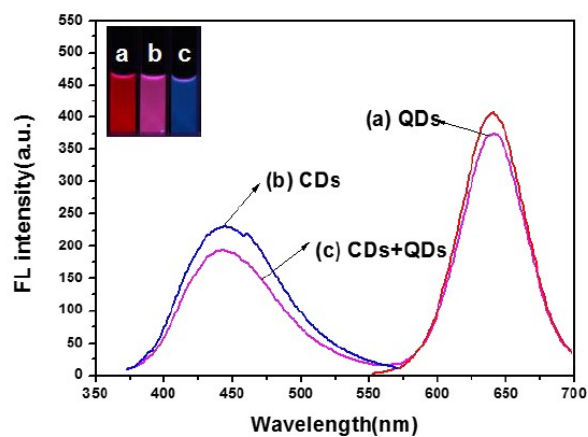


Figure S6. Fluorescent spectra of CDs and TTCA-modified CdTe QDs and the mixing TTCA-QDs/CDs at the excitation of 350 nm (the inset photos were taken under 365nm UV lamp).

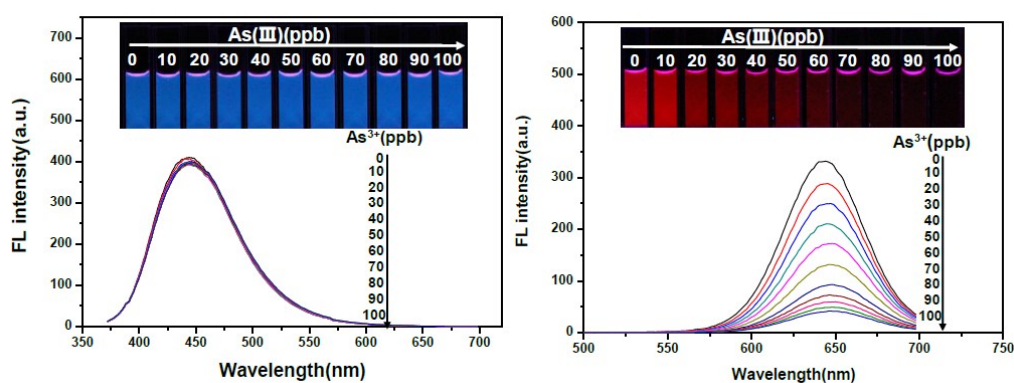


Figure S7. Fluorescent spectra of CDs (left) and TTCA-QDs (right) with the addition of As(III). The insets show the corresponding fluorescent photos under 365 nm UV lam

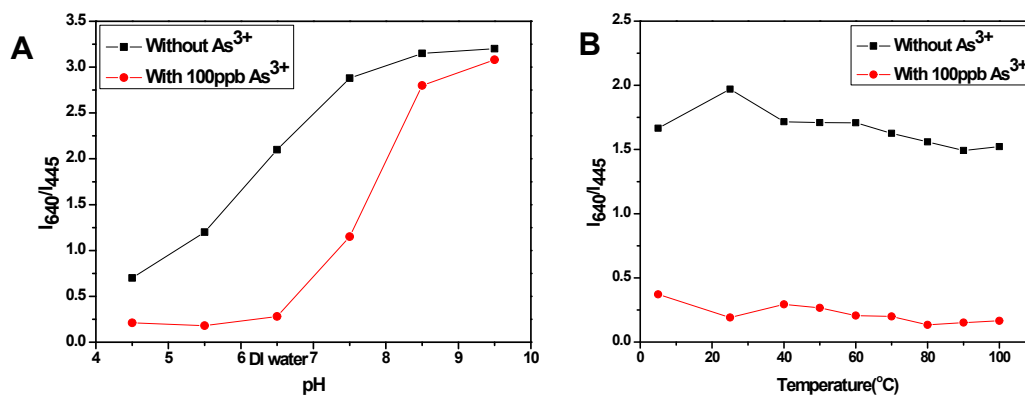


Figure S8. Effect of temperature and pH on the fluorescence intensity ratio (I_{640}/I_{445}) of the ratiometric probe in the absence (black line) and presence (red line) of 100 ppb As³⁺.

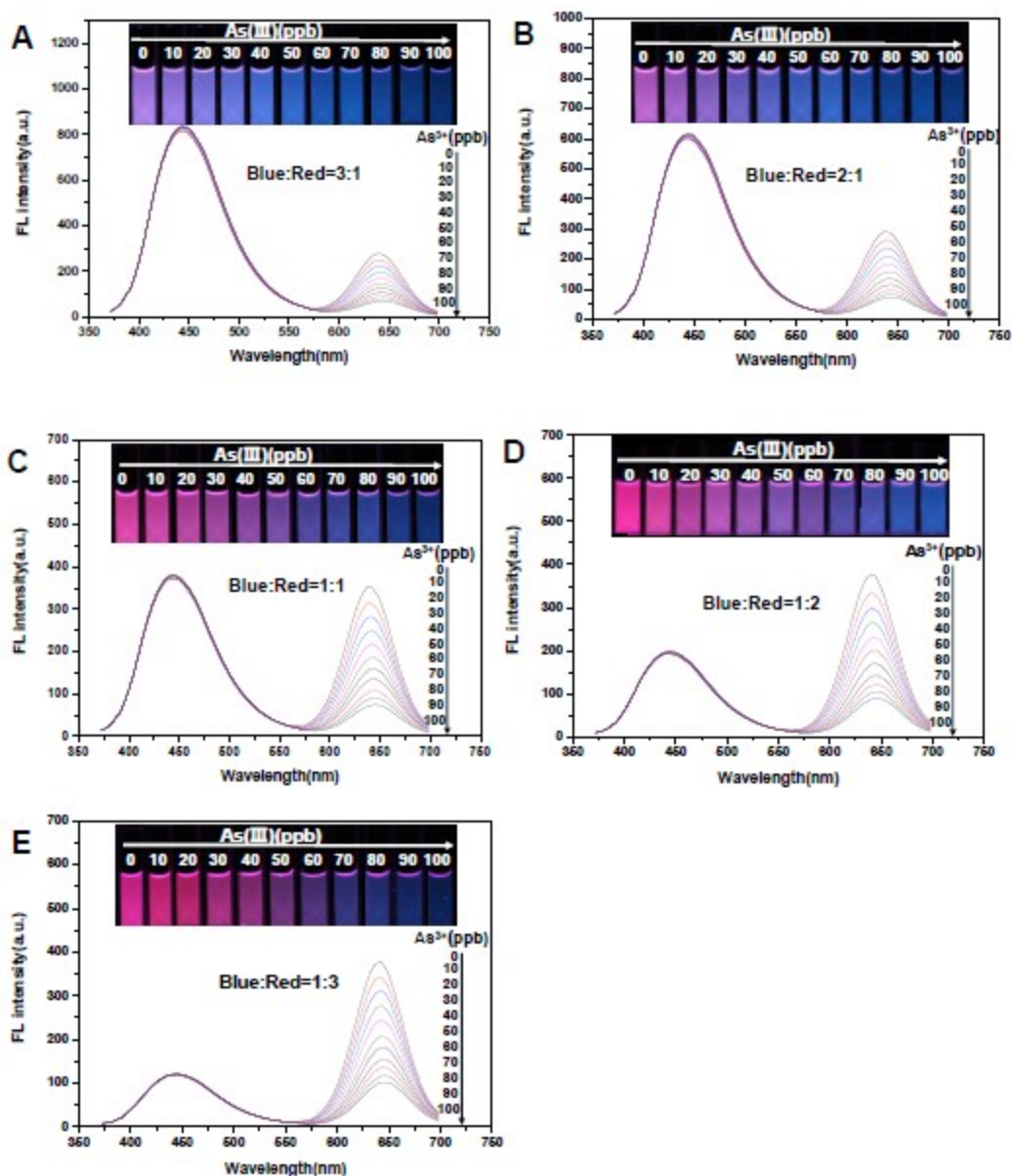


Figure S9. The fluorescent spectra of mixture of blue CDs and red TTCA-QD chains at different ratios with the addition of As(III). The ratios of fluorescent intensity (blue to red) were (A) 3:1, (B) 2:1, (C) 1:1, (D) 1:2, (E) 1:3. The insets show the corresponding fluorescent photos under 365 nm UV lamp.

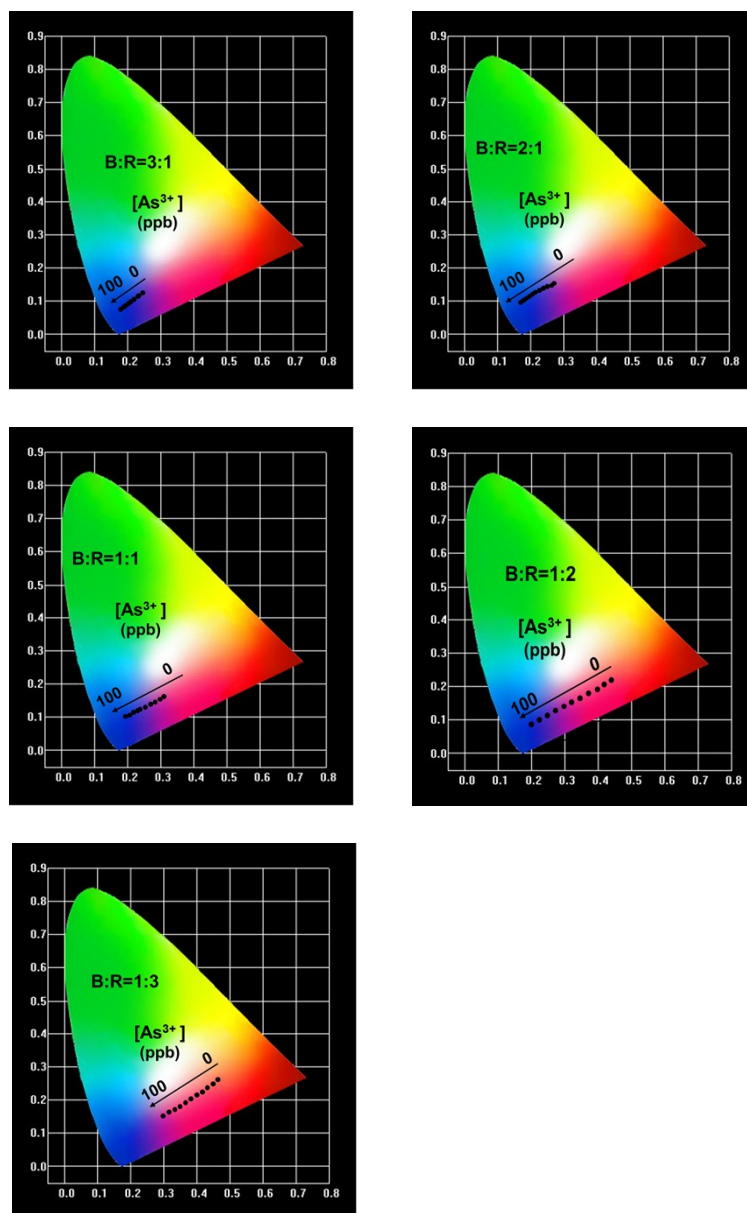


Figure S10 The chromaticity data of the optimum choice for CDs and TTCA-QD chains ratio at 3:1, 2:1, 1:1, 1:2, 1:3 respectively.

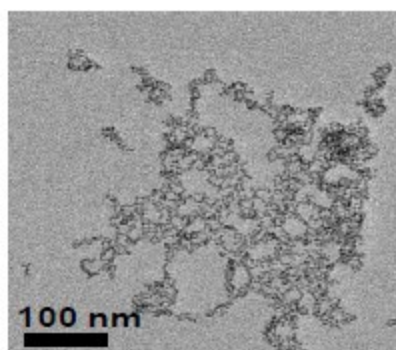


Figure S11. The TEM image of the TTCA-QDS samples after adding As³⁺

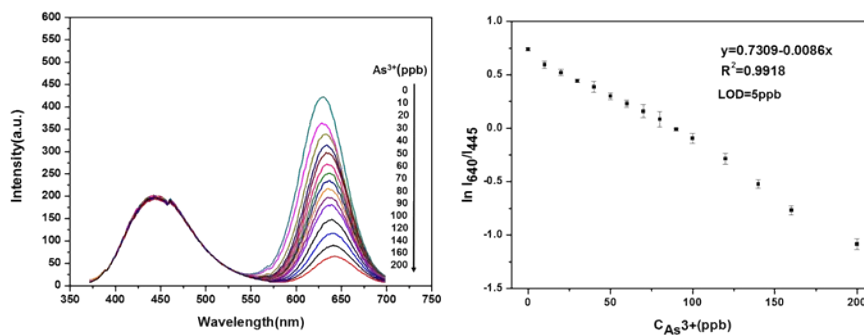


Figure S12. (A) The fluorescent spectra of mixture of blue CDs and red MPA QDs at ratios 1:2 with the addition of As(III). (B) Fluorescent intensity ratio, $\ln(I_{640}/I_{445})$, vs the concentrations of As(III) in the MPA-QDs/CDs. The LOD was 5ppb.

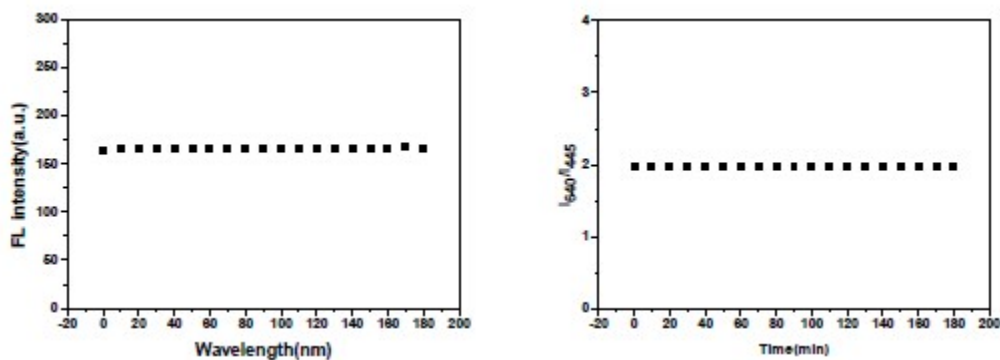


Figure S13. Photostabilities of (A) blue CDs and (B) the ratio of mixing TTCA-QDs/CDs fluorescence (at 640 and 445 nm).

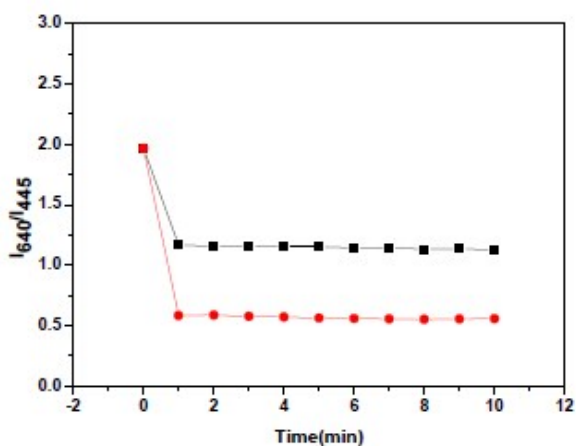


Figure S14. The dynamics of fluorescent responses of TTCA-QDs/CDs to 50 and 100 ppb As(III).

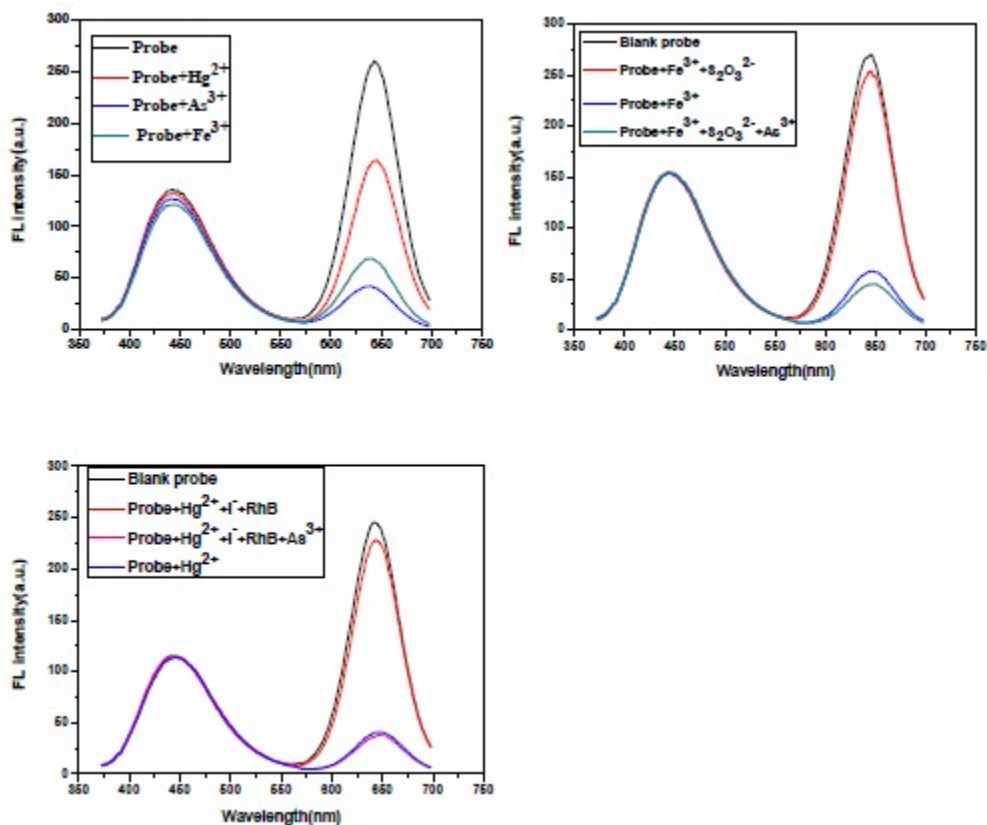


Figure S15. (a) Fluorescent responses of TTCA-QDs/CDs to Hg^{2+} , Fe^{3+} and As^{3+} (Hg^{2+} and Fe^{3+} :13.4 μM , As^{3+} :1.34 μM). (b) Fe^{3+} , $\text{Fe}^{3+}+\text{S}_2\text{O}_3^{2-}$, $\text{Fe}^{3+}+\text{S}_2\text{O}_3^{2-}+\text{As}^{3+}$ (Fe^{3+} :13.4 μM , $\text{S}_2\text{O}_3^{2-}$:134 μM , As^{3+} :1.34 μM). (c) Fluorescent responses to Hg^{2+} , $\text{Hg}^{2+}+\text{I}^-+\text{RhB}$, $\text{Hg}^{2+}+\text{I}^-+\text{RhB}+\text{As}^{3+}$. The addition of $\text{S}_2\text{O}_3^{2-}$ and I^- , RhB can effectively eliminate the interferences of Fe^{3+} and Hg^{2+} respectively.

Table S1. The comparisons of As(III) nanosensors in the previous and present works

Methods	Detection mechanism	Detection limit(ppb)	Refs
Au-Cu bimetallic	Electrochemical detection	2.09	1
Ag nanoparticles	Surface-enhanced Raman	0.76	2
Graphene oxide	Electrochemical detection	500	3
Aptamer sensor	Colorimetric/resonance scattering	40	4
Instrument	Inductively coupled plasma-mass	6.2	5
Instrument	Atomic absorption spectrometry	0.008	6
Our work	Fluorescent test paper	1	Our work

Table S2. The recoveries of As(III) in tap water and local lake water using the fluorescent measurements of TTCA-QDs/CDs probes.

Spiked concentration (ppb)	Tap water			Lake water		
	Found (ppb)	Recovery (%)	RSD (%)	Found (ppb)	Recovery (%)	RSD (%)
10	10.3	103	4.7	9.9	99	2.9
50	49.7	99.4	3.4	48.6	97.2	5.8
100	102.5	102.5	5.5	103.4	103.4	4.6

References

1. M. Yang, Z. Guo, L.-N. Li, Y.-Y. Huang, J.-H. Liu, Q. Zhou, X. Chen and X.-J. Huang, *Sensor. Actuat. B-Chem.*, 2016, 231, 70-78.
2. J. Li, L. Chen, T. Lou and Y. Wang, *ACS Appl. Mater. Inter.*, 2011, 3, 3936-3941.
3. S. Kumar, G. Bhanjanaa, N. Dilbaghi, R. Kumar and A. Umar, *Sensor. Actuat. B-Chem.*, 2016, 227, 29-34.
4. Y. Wu, L. Liu, S. Zhan, F. Wang and P. Zhou, *Analyst*, 2012, 137, 4171-4178.
5. E. Becker, R. T. Rampazzo, M. B. Dessuy, M. G. R. Vale, M. M. da Silva, B. Welz and D. A. Katskov, *Spectrochim. Acta B*, 2011, 66, 345-351.
6. C.Y. Tai, S.J. Jiang and A. C. Sahayam, *Food Chem.*, 2016, 192, 274-279.